



Springback control and plastic deformation of metal plates with large curvature in heat-assisted incremental bending process

Bo Wei¹ · Yanan Wei^{2,3} · Feifei Zhang^{2,3} · Kai He^{2,3} · Xiaobing Dang⁴ · Ruxu Du¹

Received: 17 August 2020 / Accepted: 9 December 2020 / Published online: 3 January 2021
© The Author(s), under exclusive licence to Springer-Verlag London Ltd. part of Springer Nature 2021

Abstract

With the development of the shipbuilding, chemical engineering, and military industry, the demand for bending the metal plates with large curvature is increasing dramatically. Take the shipbuilding as an example, the line heating method is widely applied. However, this traditional method has significant disadvantages. In order to improve the manufacturing efficiency and precision, a novel method called incremental bending has been presented by our team, which is based on the minimum energy principle and model-less control method. However, due to the limited formability of the metal plates at room temperature, the bending curvature of the plates during the incremental bending process cannot meet the requirements of the shipbuilding industry. Researches show that heating can reduce springback and improve the metal formability effectively. So here in this paper, a new method called heat-assisted incremental bending is presented. In this method, the metal plate is supported by several supporting pillars and the punch moves according to the loading trajectory, which is calculated by minimum energy method. In addition, the induction heating system is applied to heat the plates at the punching positions. The bending process continues step by step until the metal plate achieves the designed shape finally. During this study, the springback behavior of the metal plates during the heat-assisted incremental bending process was investigated based on theory, numerical simulation, and experiment. Then, the metal plates with large single curvature and variable curvature were deformed based on the novel thermal-mechanical coupled metal forming process. The experimental results show this new forming process can better control the [springback](#) behavior of the metal plates and achieve the objective metal plates with larger curvature with higher processing efficiency and accuracy.

Keywords Springback · Forming limit · Heat-assisted incremental bending · Curved plates

Nomenclature

w	Width of the plate	σ_0	Yield stress
R_n	Radius of curvature	t	Plate thickness
R_d	Rotation radius of supports	k	Strength coefficient
R_p	Radius of punching tool	F	Index related to anisotropy and stress/strain states
ε_{\max}	The maximum longitudinal strains	θ_1	Bending angle before springback
		θ_2	Bending angle after springback

✉ Feifei Zhang
ff.zhang@siat.ac.cn

Bo Wei
msbowei@mail.scut.edu.cn

Yanan Wei
yn.wei@siat.ac.cn

Kai He
kai.he@siat.ac.cn

Xiaobing Dang
xb.dang@zkangels.com

Ruxu Du
duruxu@scut.edu.cn

- ¹ Shien-Ming Wu School of Intelligent Engineering, South China University of Technology, Guangzhou, China
- ² Shenzhen Institutes of Advanced Technology, Chinese Academy of Sciences, Shenzhen, China
- ³ Shenzhen Key Laboratory of Precision Engineering, Shenzhen, China
- ⁴ Guangzhou Janus Biotechnology Co., Ltd., Guangzhou, China

θ_c	Punch-plate contact angle
θ_s	Springback angle of one side
ν	Poisson's ratio
θ_{st}	Total springback angle
S_1	Length of bending arc
L_d	Span of supports
n	Strain hardening exponent

1 Introduction

Bending of curved plates plays an important role in the industry development, such as shipbuilding, chemical engineering, and military industry. Generally, there are two kinds of curved plates used in various industries. Curved plates with a single curvature are commonly obtained by roll bending while curved plates with variable and multiple curvatures are usually obtained by die stamping or line heating method [1]. It should be noted, it is expensive and time consuming to manufacture the required die for stamping each curved plate, and thus die stamping method is not suitable for the small batch production. For the line heating method, the working condition is terrible and it takes much time to correct the work-piece. To overcome the problems of the traditional methods mentioned above, a lot of flexible forming methods have been proposed.

For example, Li et al. proposed multi-point forming (MPF) [2–4], which decomposes the punches and dies into a number of adjustable units. The height of each hydraulic cylinder can be changed based on the target metal plates with multiple curvatures. Compared with the traditional die stamping process, the huge cost of manufacturing target die with specific shape is reduced. However, the metal plates achieved by MPF have significant surface quality problem. In order to reduce dents and wrinkles, Wang et al. optimized the globular hydraulic cylinder head to flexible squared one based on MPF, which increases the contact area between the stamping tool and the metal plate [5]. Generally, the forming force and springback behavior of the curved plates during MPF are quite large and the formability is low. In order to decrease the forming force, Luo et al. presented cyclic multi-point incremental forming method (CMPIF) [6]. In the CMPIF process, only one punch moves a small step at each load time, and all of the punches load circularly until the objective part is achieved. Obviously, this method is complex and time consuming. To sum up, the springback prediction and control are not very well resolved through the above cold-forming methods.

Our team has been working on metal forming processes for a long time. For reducing forming force, improving the processing efficiency and forming accuracy, the incremental punching forming and incremental bending were proposed to achieve thin plates and thick plates, respectively [7–9]. For this flexible incremental bending process, the bending trajectory is calculated by beam bending minimum energy

principle. So far, the prototypes with different maximum loading forces have been designed and manufactured. Some metal plates with small curvatures have been obtained based on this incremental bending method [9, 10]. However, it is found that the deformed metal plates with large curvature cannot meet the requirement due to the huge springback behavior and low formability of the curved plates during the whole process.

Review of the previous metal forming methods reflects that the springback and low formability are the common defects of metal plates in sheet metal forming processes. In recent decades, many scholars have carried out researches on how to improve the springback prediction and reduce the springback behavior. For example, Wang et al. proposed a mathematical model base on plane-strain bending of sheet and plate and they developed a computer code called “BEND” to simulate the air bending and die bending processes [11]. Xi et al. developed an analytical model to predict the springback in air bending of advanced high-strength steels and the accuracy of the model was validated by the experimental results [12]. Fayiz et al. used the Kriging metamodel approach to predict the springback behavior of the metal plates in the air bending process [13]. It should be noted that only the middle position of the sheet was investigated in the above methods. The springback behavior of sheet metal at different punching positions must be studied for the 3D free form metal plates. To reduce springback, lots of localized and global heating methods, including laser-assisted incremental forming [14], electric hot incremental forming [15], air blowers hot incremental forming [16], and fluid hot incremental forming [17], have been applied to heat the metal sheet during the forming process. For the incremental bending process, the proper heating method is necessary to use to reduce the springback behavior of the metal plates with large curvature.

In order to improve the formability of the metal plates, lots of studies have been carried out in recent years. For example, Gisario et al. adopted external force laser-assisted bending method to achieve the bending angles from over 80° to about 140° for titanium alloy, from about 90° to about 140° for aluminum, and from over 70° to 140° for AISI 304 stainless steel [18]. Roohi et al. obtained the 90° bending angle for Al-5005 alloy with thickness of 5 mm [19]. During this method, the metal sheets must be clamped by a custom-built device in the forming process, which increases the cost and limits the application for complex metal forming. So the die-less heat-assisted incremental bending process is very necessary for achieving the metal plates with large and complex curvature.

Here, in this paper, the heat-assisted incremental bending method is presented. The bending behavior of the metal plates in the heat-assisted incremental bending is investigated based on theoretical analysis, numerical simulations, and experiments. The new heat-assisted incremental bending method is validated by forming the metal plates with large curvatures based on the springback law and minimum energy method.

The rest of the paper is organized as follows: the heat-assisted incremental bending theory is presented in Section 2. Section 3 gives the experimental procedure and corresponding numerical simulation. Section 4 discusses and analyzes the experimental results and validation of the numerical simulation. Finally, Section 5 contains conclusions.

2 Heat-assisted incremental bending theory

2.1 Heat-assisted incremental bending system-working principle introduction

Heat-assisted incremental bending is one flexible and die-less forming process for manufacturing different types of metal plates. As shown in Fig. 1, the metal plate is supported by several supporting pillars. Each supporting pillar has a rotating head for accommodating the bending of the metal plate. As the punching tool moves down to press the metal plate, plastic

deformation occurs around the punch point when the local stress exceeds the yield limit of the metal plate during the incremental bending process. To achieve the objective metal plate shape, the incremental bending method is carried out by continuous bending operations. In each bending operation, the metal plates are punched at different punching position with different punching depths. At the same time, the induction heating system is applied to heat the plates at the punching positions. The bending process continues step by step until the metal plate achieves the designed shape finally.

Based on forming principle shown in Fig. 1, three incremental bending prototypes with different maximum punching forces have been designed (Fig. 2). As shown in Fig. 3, the machine tool used for this study is composed of a punching tool, 4 × 3 supporting pillars, a control system, and a visual inspection system. In the heat-assisted incremental bending study, a robot and an induction heating system are also introduced. The dimension of the machine is 1750 mm × 1750 mm × 1950 mm and the kinematic accuracy is ± 0.005 mm. The

Fig. 1 Schematic illustration of heat-assisted incremental bending process

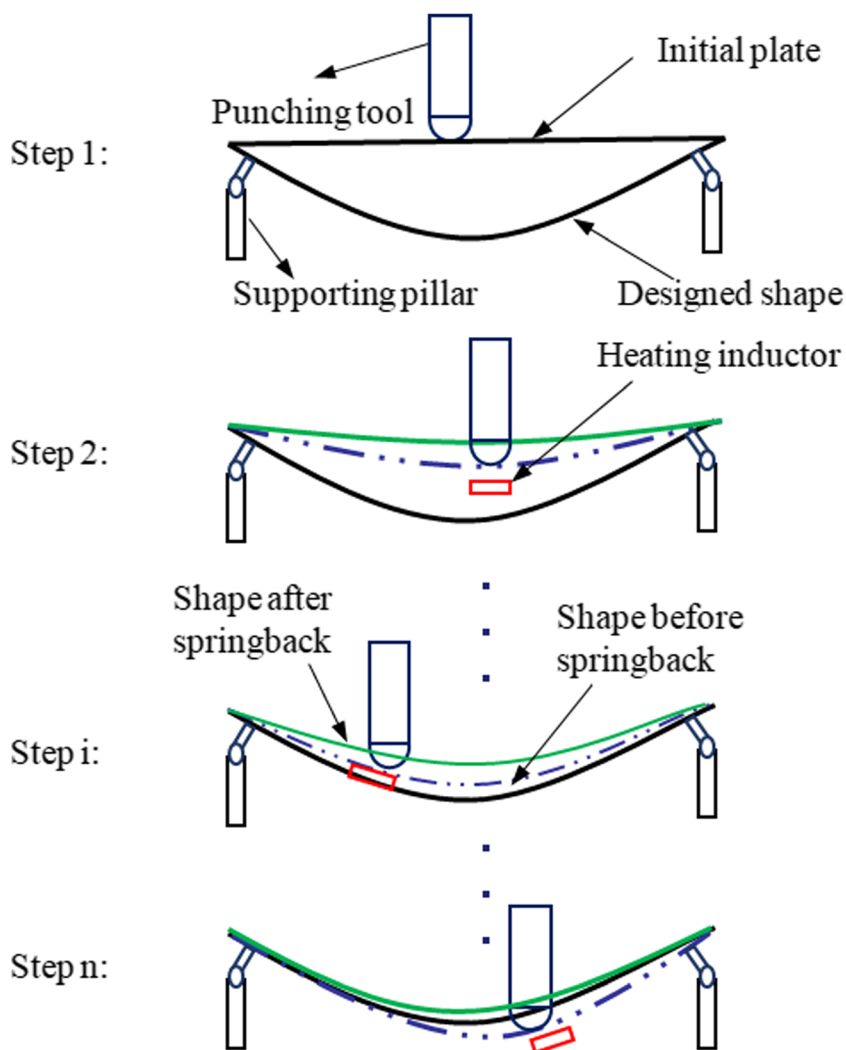


Fig. 2 Prototype machines: **a** maximum punching force 20 kN, **b** maximum punching force 50 kN, **c** maximum punching force 6000 kN

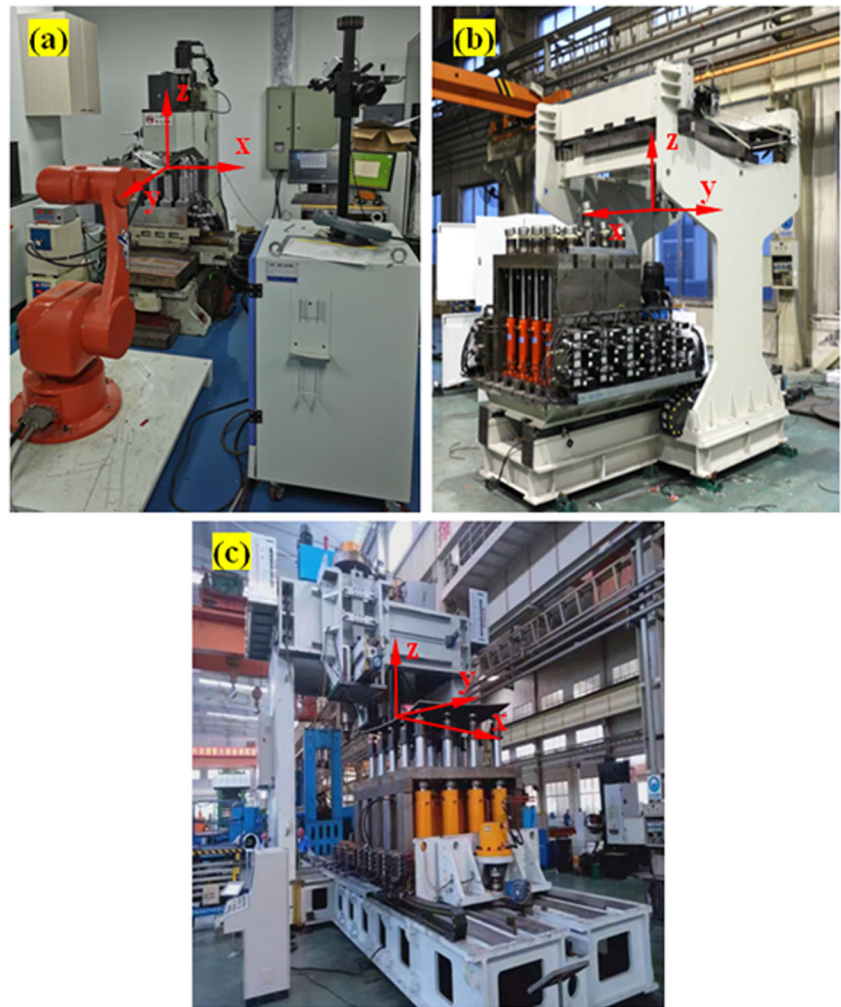
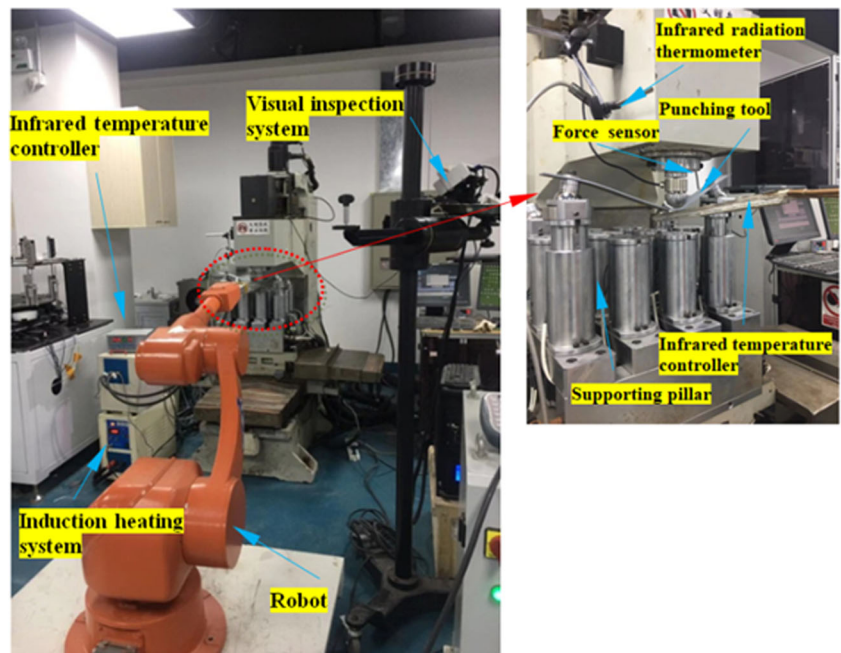


Fig. 3 Experimental setup of the heat-assisted incremental bending process



maximum punching force is 20 kN and the working stroke of the punching tool is 500 mm in z direction. The supporting pillars can move along x -axis and y -axis, with the corresponding working stroke of 500 mm and 400 mm, respectively. To accommodate the bending of the sheet metal plate, each pillar has a rotatable head. The metal plate is fixed on the rotatable head by screws or electromagnets. The visual inspection system is used to measure the shape data of work-piece. The induction heating system includes high frequency induction heating equipment, infrared temperature controller, and an infrared radiation thermometer. The robot is used to clamp the infrared temperature controller to keep the inductor heating the plate continuously.

2.2 Loading path generation—minimum energy principle

The loading trajectory is very important for achieving the target metal plates with better surface quality and less processing time during the metal forming process. In our previous study [9], the metal plate was discretized into a series of strips, and each strip can be modeled as a beam. The minimum energy principle based on Euler-Bernoulli beam theory was applied to obtain the incremental loading trajectory. As shown in Fig. 4, E is the error point between the designed shape and current shape. During the incremental bending process, the supporting points are at the two ends while the punching point is at the largest error point. For this novel heat-assisted incremental bending process, the elastic-plastic deformation rule of the curved plates is influenced by the heating temperature, and thus, the optimal loading path can be changed accordingly.

2.3 Elastic-plastic-thermal bending deformation theory of the metal plates

The springback behavior of the metal plates is caused by elastic recovery and it is an unavoidable phenomenon in metal

forming processes. In the heat-assisted incremental bending process, a number of bending steps should be carried out, and after each step, there is springback phenomenon. In order to obtain the better forming accuracy, the springback behavior of the metal plates at each step should be taken into account. Many studies have been conducted on springback, while most studies focus on the press-brake bending such as air bending, V-die bending, and U-die bending. In the press-brake bending process, the punching position is only at the mid-span of the sheet. However, in the heat-assisted incremental bending process, the punching position is constantly changing based on the minimum energy principle. So, the springback behavior of the metal plates at different punching positions must be investigated.

In this paper, the ratio of width to thickness (w/t) of the metal plate is greater than 8, so the plain-strain bending deformation mode is used to analyze the springback behavior of the metal plates during the heat-assisted incremental bending.

The basic bending model used for heat-assisted incremental bending analysis is shown in Fig. 5. The coefficient α is applied to describe the different stamping positions in the incremental bending process. In this model, true strain hardening and normal anisotropy of the plate are taken into consideration. The Swift's exponential hardening model ($\bar{\sigma} = k(\varepsilon_0 + \bar{\varepsilon})^n$) and Hill's 48 yield criteria [20] are selected to describe the material property and yield behavior, respectively. It should be noted that the basic mechanical properties of the material changes with the heating temperature. So the elastic-plastic bending deformation behavior of the material changes accordingly. The yield value of stress (σ_0) decreases with increasing the temperature. In addition, several assumptions are considered in the incremental bending deformation analysis model. These assumptions include (1) the thickness of the plate is constant during the whole process; (2) the bending moment distribution is linear along sheet length; (3) as shown in Fig. 5, the plate can be divided into six deformation regions along the length in the incremental bending process:

Fig. 4 Schematic illustration of the punching and supporting points

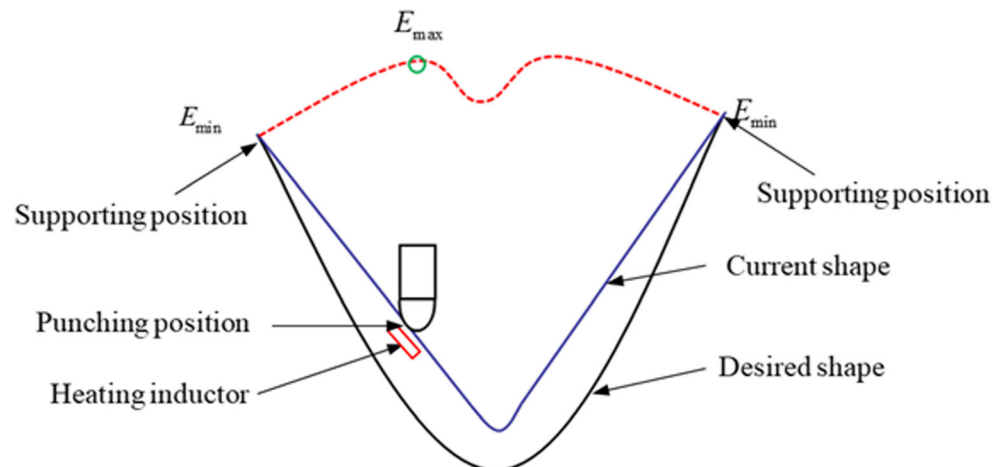
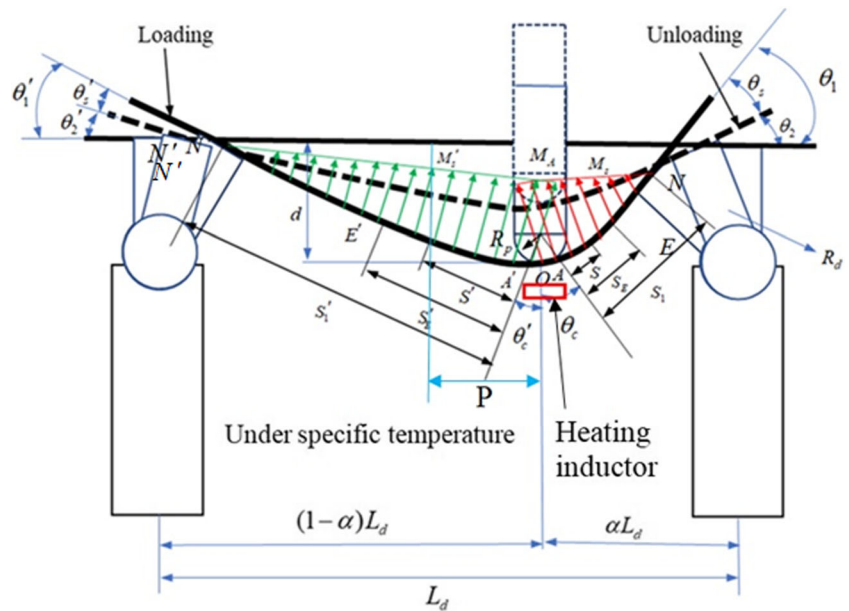


Fig. 5 Geometric relationship and coordinate system for bending at specific temperature



OA and OA' , the punch-plate contact region, are the fully plastic bending deformation zones, AE and AE' are the elastic-plastic bending deformation zones, and EN and EN' are the elastic bending deformation zones.

For the elastic bending zone, the bending moment M_e is found as

$$M_e = w \int_{-\varepsilon_x}^{\varepsilon_x} \sigma_x y dy = \frac{2wR_n^2 E'}{3} \varepsilon_x^3 \quad 0 \leq \varepsilon_x \leq \varepsilon_e \quad (1)$$

The bending moment for fully elastic bending, M_E , can be calculated as shown in

$$M_E = w \int_{-\varepsilon_e}^{\varepsilon_e} \sigma_x y dy = \frac{wt^2 \sigma_0}{6E'} \quad (2)$$

And for the elastic-plastic bending process, the bending moment M_{ep} is comprised of the elastic moment M_e and the plastic moment M_p

$$M_p = 2w \int_{\varepsilon_e}^{\varepsilon_{\max}} \sigma_x y dy = 2wkF^{n+1} R_n^2 e^{2(\varepsilon_e - \varepsilon_0)/F} \sum_{j=0}^{\infty} \left\{ \frac{2^j - e^{2(\varepsilon_e - \varepsilon_0)/F}}{(j+1+n)j!} \times [(\varepsilon_{\max} + (\varepsilon_0 - \varepsilon_e)/F)^{j+1+n} - (\varepsilon_0/F)^{j+1+n}] \right\} \quad (3)$$

Then,

$$M_{ep} = M_e + M_p \approx \frac{2}{3} \varepsilon_e^2 \sigma_0 w R^2 + \frac{2wKF^{n+1}}{n+2} \left(\frac{t}{2}\right)^{n+2} / R^n + \frac{3wKF^{n+1}}{n+3} \left(\frac{t}{2}\right)^{n+3} / R^{n+1} \quad (4)$$

For the fully plastic bending, the maximum bending moment, M_A , can be obtained by neglecting the ε_e in Eq. (3)

$$M_A = 2wkF^{n+1} R_n^2 e^{-2\varepsilon_0/F} \sum_{j=0}^{\infty} \left\{ \frac{2^j - e^{2\varepsilon_0/F}}{(j+1+n)j!} \times [(\varepsilon_{\max} + \varepsilon_0/F)^{j+1+n} - (\varepsilon_0/F)^{j+1+n}] \right\} \quad (5)$$

For the springback behavior analysis, the curvature change before and after springback can be defined as follows.

$$\frac{1}{r} - \frac{1}{r'} = \frac{M}{E'I} = \frac{12M(1-\nu^2)}{wt^3 E} \quad (6)$$

As far as the springback angle be concerned,

$$\Delta\theta_s = \Delta S \left(\frac{1}{r} - \frac{1}{r'} \right) = \frac{M}{E'I} dS \tag{7}$$

where $\frac{1}{r}$ is the curvature of the plate in bending, $\frac{1}{r'}$ is the curvature of the plate after the bending moment is removed, E' is the plane-strain modulus ($E' = E/(1 - \nu^2)$), I is the second moment of area about the middle axis ($I = wt^3/12$), and the dS is the length of a small element of the plate.

The springback consists of two components, which are the springback in punch-sheet contact zone and springback along the bending arm. The springback angles, θ_s and θ'_s , can be calculated by Eqs. (8–9).

$$\begin{aligned} \theta_s &= \int_0^{S_1} \frac{1}{4} \frac{M(S)}{E'I} dS + \int_0^{l_1} \frac{1}{4} \frac{M_A}{E'I} dl = \frac{1}{4} \frac{M_A}{E'I} (S_1 + l_1) \\ &= \frac{3}{2} \frac{KF^{n+1}}{2+n} \frac{1}{E'} \left(\frac{t}{2R_p + t} \right)^n \left(1 + \frac{3n+2}{2n+3} \frac{t}{2R_p + t} \right) \frac{S_1 + l_1}{t} \end{aligned} \tag{8}$$

$$\begin{aligned} \theta'_s &= \int_0^{S'_1} \frac{1}{4} \frac{M(S')}{E'I} dS + \int_0^{l'_1} \frac{1}{4} \frac{M_A}{E'I} dl = \frac{1}{4} \frac{M_A}{E'I} (S_1 + l'_1) \\ &= \frac{3}{2} \frac{KF^{n+1}}{2+n} \frac{1}{E'} \left(\frac{t}{2R_p + t} \right)^n \left(1 + \frac{3n+2}{2n+3} \frac{t}{2R_p + t} \right) \frac{S_1 + l'_1}{t} \end{aligned} \tag{9}$$

The total springback angle, θ_{st} , is expressed as

$$\theta_{st} = \theta_s + \theta'_s \tag{10}$$

Based on the geometrical relationship in Fig. 5, the punch stroke, d , can be expressed as

$$\begin{aligned} d &= \int_0^{S_1} \sin \theta dS + [R_d - (R_d + t/2) \cos \theta_1] \\ &\quad + [R_p - (R_p + t/2) \cos \theta_c] + t \end{aligned} \tag{11}$$

The springback height of the punching position, h , can be calculated

$$h = d - [R_d(1 - \cos \theta_2) + (\alpha L_d - R_d \sin \theta_2) \tan \theta_2] \tag{12}$$

With the increase of the heating temperature, the yield stress σ_0 and elastic modulus of the mild steels decrease, and thus, the maximum bending moment M_A and the springback angle θ_s decrease accordingly. Therefore, the bending angle after springback $\theta_2 = \theta_1 - \theta_s$ increases. As a result, the springback height shown in Eq. 12 decreases accordingly.

3 Experimental and numerical simulation study

3.1 Experimental study of the strip in heat-assisted incremental bending process

For this experiment, the forming force at various stamping positions and temperatures should be taken into consideration. The forming force should not exceed the nominal force of the machine tool, and the springback law of the metal plates during the heat-assisted incremental bending process should be investigated to better control the whole deformation process. So the target of the experimental study is to find out the deformation rule including the forming force rule and springback law under different forming factors.

The mild steel Q235 is used in this experiment. The mechanical properties and the thermal properties of the mild steel at different temperatures are listed in Tables 1 and 2 [21]. The dimension of the plate used in this experiment is 440 mm × 38 mm × 3 mm. As shown in Fig. 3, during the experiments, the metal plates were fixed on the supporting cylinders by two screws to prevent the metal plates from sliding, and the infrared radiation thermometer was used to measure the temperature at the punching position. The feed speed of the stamping tool was 100 mm/min. The forming force was recorded by force sensor during the whole process. The experimental arrangement is listed in Table 3 and the corresponding experimental samples are shown in Fig. 6. Besides the room temperature, other two temperatures, 250 °C and 500 °C, are chosen in the experiment process. Three different punching positions (0 mm, 30 mm, and 60 mm) from the center are adopted in the experiment process. The experimental setup and the schematic diagram are given in Figs. 3 and 5 (where P is the distance between the punching position to the center of the plate), respectively. For each experimental state, the 3D optical scanning system was applied to obtain the metal plates' shape before and after unloading to analyze the springback behavior during the heat-assisted incremental bending process.

3.2 Numerical simulation study of the strip in heat-assisted incremental bending process

Nowadays, finite element simulation has been widely used to investigate the metal plates' deformation behavior during various forming processes. The numerical simulation shown in this study is based on the general commercial finite element software.

To obtain the accurate simulation results, it is very important to select the appropriate finite element analysis method. Generally speaking, two methods, the dynamic explicit method and static implicit method, are usually applied for analyzing punching process and springback process, respectively.

Table 1 Mechanical properties of mild steel [21]

Temperature (°C)	Elasticity modulus (N/mm ²)	Poisson's ratio	Expansion	Yield stress for $e_p = 0$ (N/mm ²)	Yield stress for $e_p = 0.1$ (N/mm ²)
20	0.206E+06	0.296	0.117E-04	344.64	422.64
100	0.203E+06	0.311	0.117E-04	331.93	409.93
200	0.201E+06	0.330	0.122E-04	308.30	386.30
300	0.200E+06	0.349	0.128E-04	276.07	342.57
400	0.165E+06	0.367	0.133E-04	235.22	290.22
500	0.120E+06	0.386	0.144E-04	185.77	230.77
600	0.600E+05	0.405	0.148E-04	127.71	162.71
700	0.400E+05	0.423	0.148E-04	68.55	96.05
800	0.300E+05	0.442	0.148E-04	64.35	84.35
900	0.200E+05	0.461	0.148E-04	46.65	60.65

However, for this heat-assisted incremental forming process, the feed speed of the stamping tool is 100 mm/min, and the bending process can be regarded as quasi-static deformation. In addition, for the experimental cases with several incremental steps, successive punching-springback processes are conducted; thus, it is not convenient to change the finite analysis methods over and over again. Besides, there is significant dynamic effect if using the dynamic explicit method to simulate the incremental bending process since the constraint condition is quite limited. Therefore, the static implicit method is selected for the whole simulation process.

In this simulation study, the elastic-plastic-thermal coupled constitutive model is used. Von Mises isotropic yield criteria is used to describe the yielding behavior of the mild steel Q235, and the bilinear stress-strain curve lines, decided by the mechanical properties shown in Table 1, are used to describe the stress-strain behavior of the mild steel Q235 under different temperatures. Meanwhile, the rigid model is used to describe the tools. As shown in Fig. 7, the numerical model is composed of one metal plate, one punch (the diameter is 50 mm), and two rotatable supporting pillars. The dimensions of all the strips in the numerical simulation and experiments are the same (460 mm × 38 mm × 3 mm). In the finite element numerical model, the full integrated shell element is used to mesh the strip. The metal plate can rotate around the mass

center of the supports with the rotation radius of 42 mm. Besides, the one way surface to surface contact method is chosen to define the contact between the strip and the tools.

Three different kinds of mesh sizes (2 mm, 4 mm, and 6 mm) are used for calculation. For all the three cases, five integration points are defined for the shell elements. The calculation times for the three cases are 5 min, 3 min, and 2 min, respectively. The predicted stamping forces are compared with experimental ones (as shown in Fig. 8). It can be seen that for the simulation cases with mesh sizes of 2 mm and 4 mm, the predicted stamping forces coincide well with the experimental data. However, for the case with mesh size of 6 mm, the predicted stamping force is seriously distortion. So, considering both the accuracy and efficiency, the optimal mesh size for the strip is 4 mm.

3.3 Springback behavior and force analysis of the strip under different heating temperatures

As shown in Fig. 3, the force sensor was installed on the punching tool to measure the forming force during the incremental bending process. Figure 9 illustrates the reported forming force-punching depth curves at different punching positions and temperatures, respectively. Results show that there is a good consistency between the numerical simulation

Table 2 Thermal properties of mild steel [21]

Temperature (°C)	Thermal conductivity (W/mm/°C)	Specific heat (kJ/kg/°C)	Temperature (°C)	Thermal conductivity (W/mm/°C)	Specific heat (kJ/kg/°C)
0	51.9E-3	486	500	39.4E-3	557
100	51.1E-3	486	600	35.6E-3	586
200	48.6E-3	498	700	31.8E-3	619
300	44.4E-3	515	800	26.0E-3	691
400	42.7E-3	536	900	26.4E-3	695

Table 3 Experimental arrangement

Number	Punching position (mm)	Punching depth (mm)	Temperature (°C)
Case 1	0	60	20
Case 2	0	60	250
Case 3	0	60	500
Case 4	30	60	20
Case 5	30	60	250
Case 6	30	60	500
Case 7	60	60	20
Case 8	60	60	250
Case 9	60	60	500

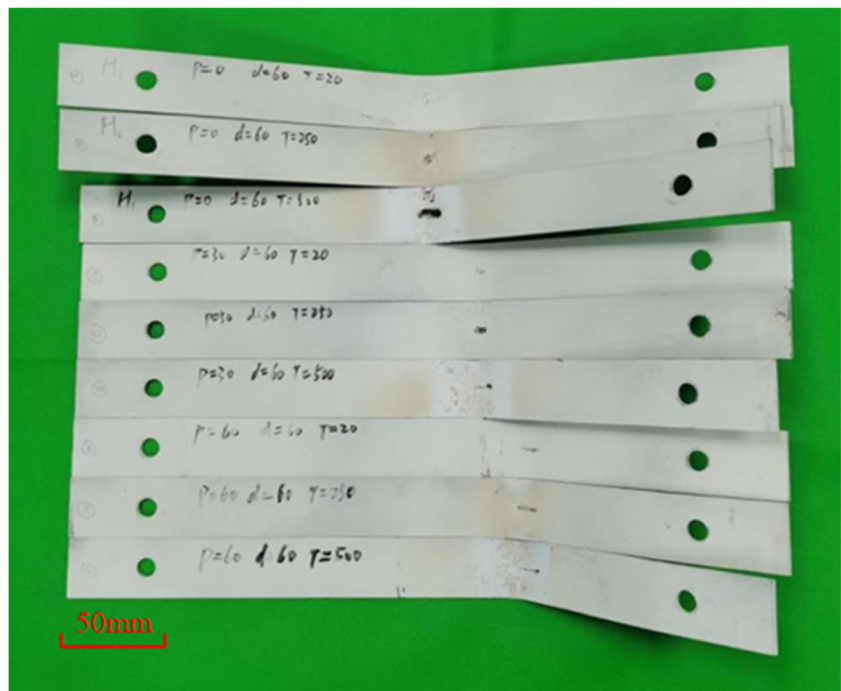
results and experimental results. The maximum discrepancy is about 10%. The discrepancy can be attributed to the errors in sample preparations and signal measurements in the experimental process, and the ignorance of shear stress in the numerical simulation process. In addition, it is revealed that the tendency of the forming force during the bending processes under different conditions is quite similar. That is, the forming force increases first with the punching depth, then the forming force becomes stable, and last, the forming force decreases. That is because at the beginning of incremental bending process, the elastic deformation occurs, and the elastic bending moment increases quickly with the increasing punching depth. As a result, the forming force increases accordingly. Then, the bending moment increases slowly when the plastic

deformation occurs in the vicinity of the punch tip. Therefore, the forming force increases to the maximum value slowly until the bending moment reaches to maximum when the full plastic deformation occurs in the vicinity of the punch tip. As plastic hinge occurs, the bending moment does not increase anymore, so the forming force becomes stable correspondingly. However, the decrease in forming force due to the plastic deformation resistance decreases with increasing plastic deformation region continually. Moreover, Figure 9 also shows that the maximum forming force during the bending process increases with bigger punching distance (*P*) due to the bigger bending moment.

In addition, it is also shown that the forming force decreases with raising the temperature. And the higher the temperature is, the more the forming force decreases. It is due to the fact that increasing the temperature can reduce the materials' yield limit and thus reduce the bending moment accordingly. However, according to the previous experimental study, the punching depth has no obvious effect on the forming force and springback behavior in the same temperature. In addition, the forming force can decrease to 0 in punching position 60 mm when the punching depth is 60 mm and the temperature is 500 °C.

Figure 10 shows the springback heights of the strips at different stamping points and different temperatures based on theoretical analysis, experiments, and numerical simulation. Results show that the springback heights of the strips decrease with the increasing temperature for all the three methods. The theoretical springback values overestimate the

Fig. 6 Experimental samples



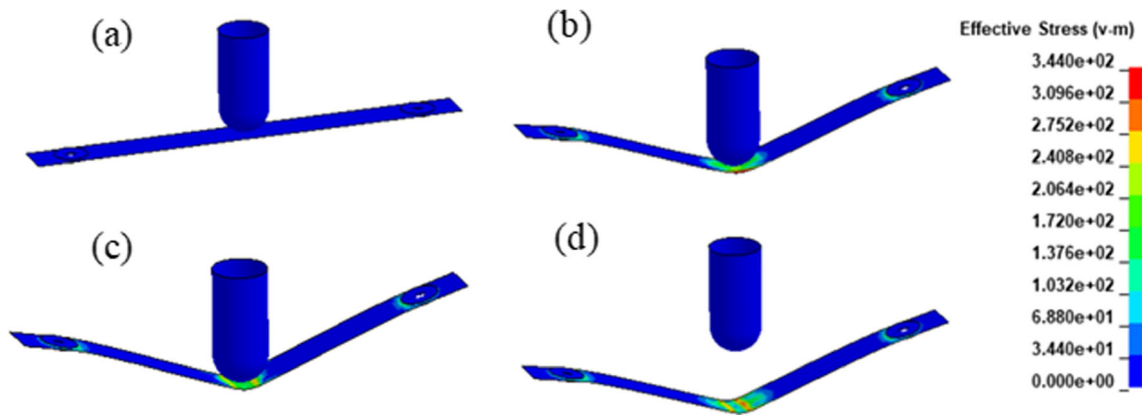


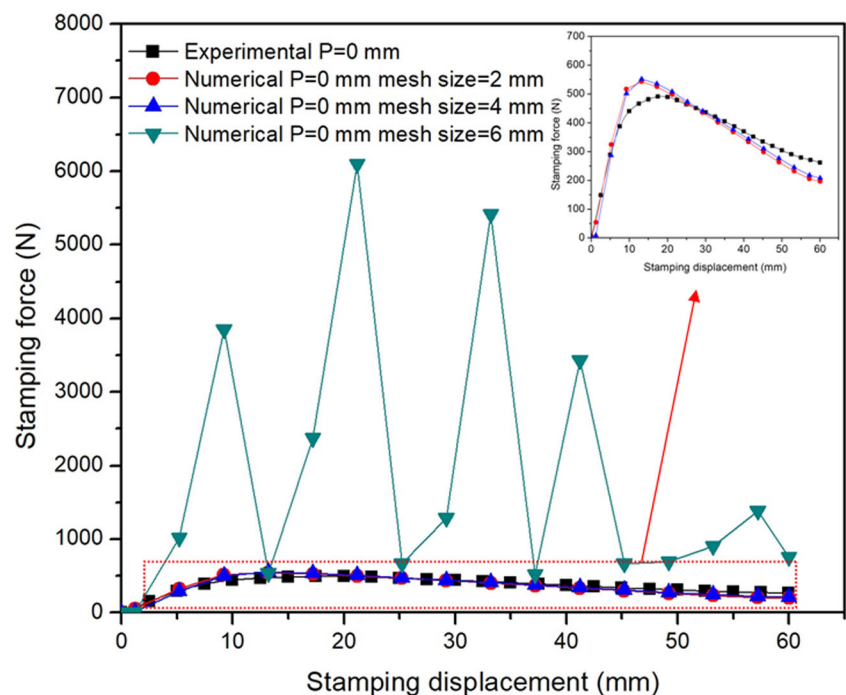
Fig. 7 Numerical simulation models at various states. **a** Initial state, **b** punching state, **c** heating state, and **d** springback state

experimental results with the maximum discrepancy of about 12%. It can be attributed to the fact that the analytical model shown in Section 2.3 (Eq. 12) is calculated with simplified assumptions in material, geometry model, and bending process. However, the numerical simulation results coincide well with the experimental results. Based on the data of Figure 10, the springback heights for different positions at different temperatures can be obtained, which helps to obtain the shape of the plate after each springback process and then achieve the proper loading path. It should also be noted that the springback heights at 500 °C are smaller than 2 mm, so the springback behavior is almost eliminated. So, following the above study, the optimal temperature 500 °C with minimum springback height is applied for the incremental bending process.

3.4 Experimental study of the curved plates in heat-assisted incremental bending process

Here, the single curvature plate and variable curvature plate are selected as the target shapes. The design of the large single and variable curvature part is shown in Figs. 11 and 12, respectively. In this study, the single curvature plate and the variable curvature plate are discretized into three paralleled strips along x direction. As shown in Figs. 13 and 14, the loading trajectories were calculated based on the springback law at 500 °C and minimum energy principle. The dimension of the plate used in this experiment is 460 mm × 330 mm × 3 mm. Four screws and two electromagnets were used to fix the metal plate on the supporting cylinders.

Fig. 8 Influence of mesh size on stamping force



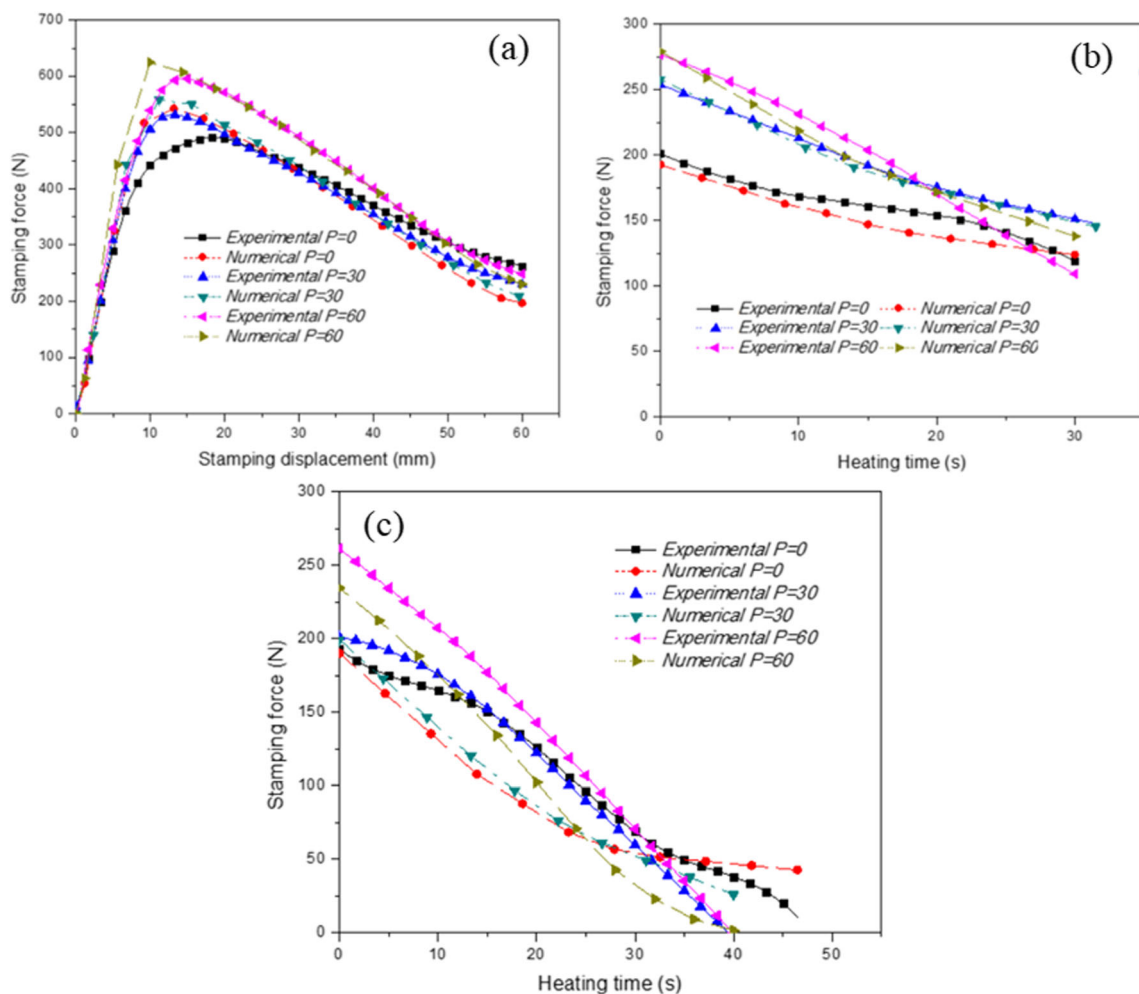


Fig. 9 Forming force with the change in punching position using experimental and numerical methods with the stamping displacement of 60 mm under different temperatures, **a** 20 °C, **b** 250 °C, and **c** 500 °C

Figure 15 shows the actual experimental states. First, the punching tool moved down to press metal plate to the specific depth at the punching position, then the punching position was heated linearly to the designed temperature by the heating inductor, and finally, the punching tool moved back after the heating process was completed.

3.5 Numerical simulation study of metal plates with large curvature in heat-assisted incremental bending process

For this study, the deformation process of the metal plates with both large single curvature and large variable curvature is simulated. Here, taking the numerical simulation of the metal plate with large variable curvature as an example, the simulation parameter settings are described as follows: the basic simulation parameter settings (including the material models used for the metal plate and the tools, the punching speed, and the control setup) are the same as that used for the

strip shown in Section 3.2. However, the numerical model is composed of one metal plate, one punch, and six supporting pillars. The dimensions of all the metal plates in the numerical simulation and experiment model are the same (460 mm × 330 mm × 3 mm). And the metal plates are meshed with full integrated shell element. Since the hourglass can be completely eliminated by using full integrated element, there is no hourglass control in the simulation. Besides, the coulomb friction law is used to describe the frictional behavior between the tools and the plate. During the simulation process, the punching tool moves to the target positions following the loading trajectory as shown in Fig. 16. When the punch moves down along z direction, the objective temperature is loaded at the punching position region of the metal plate. For the simulation of the metal plates with large variable curvature, the calculation time is about 2 hours. Figure 17 shows the whole simulation process, including the initial state, punching state, heating state, and springback state.

Fig. 10 Springback law under various temperatures

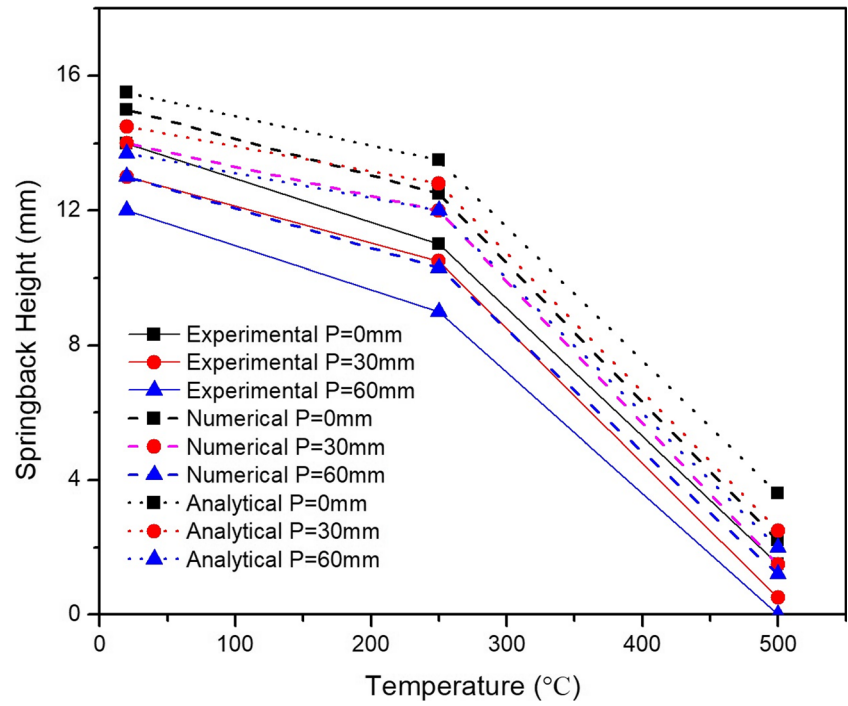


Fig. 11 Large single curvature metal plate bending: **a** designed surface. **b** Curve of a strip

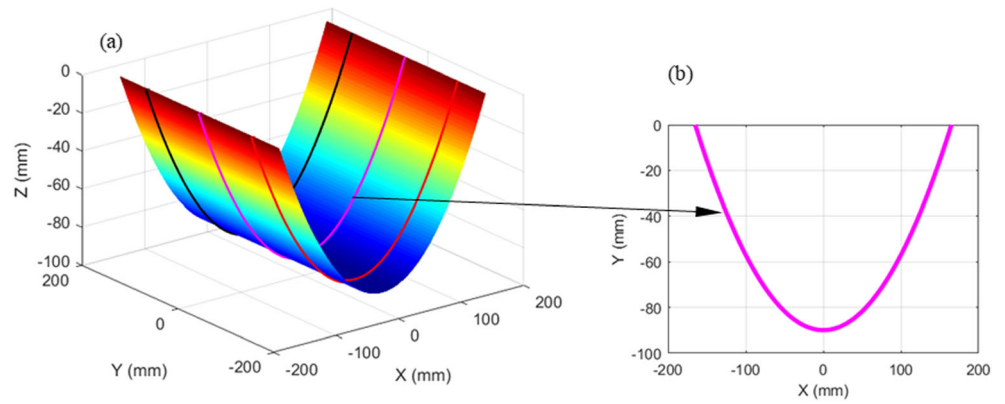


Fig. 12 Large variable curvature metal plate bending: **a** designed surface. **b** Curve of strips.

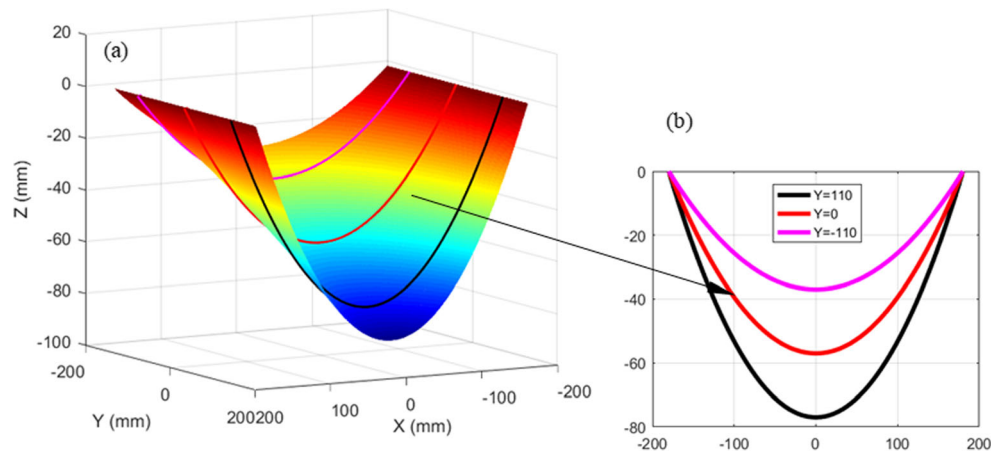


Fig. 13 Punching trajectory for large single curvature metal plate

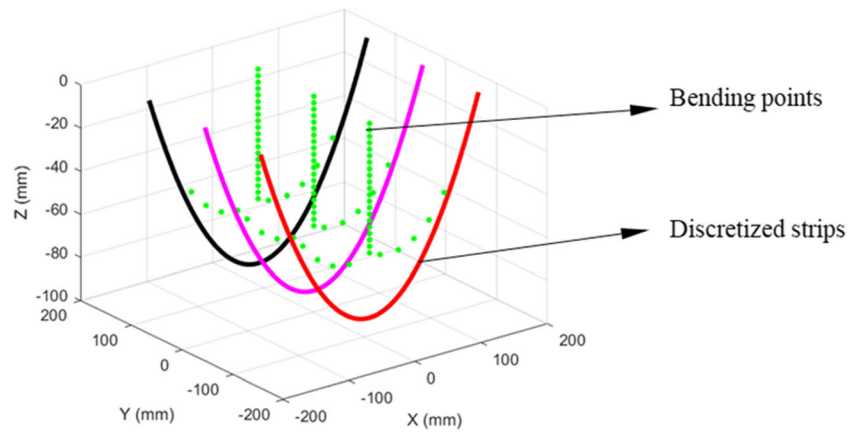
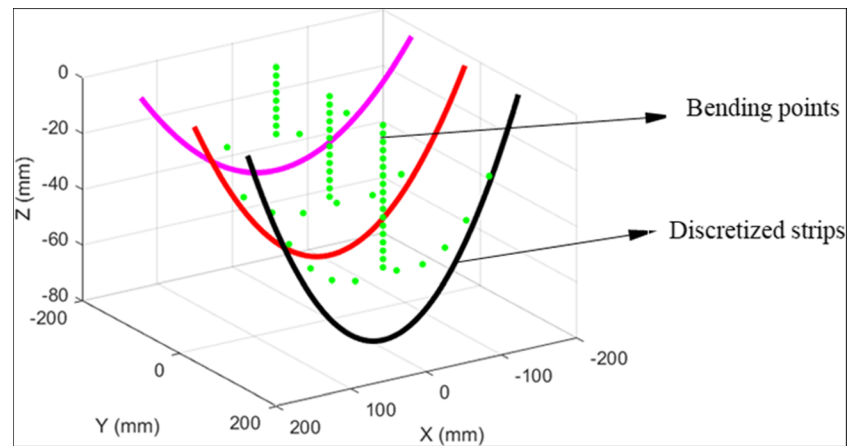


Fig. 14 Punching trajectory for large variable curvature metal plate



4 Results and discussion

4.1 Analysis on the deformation behavior of metal plates with large single curvature

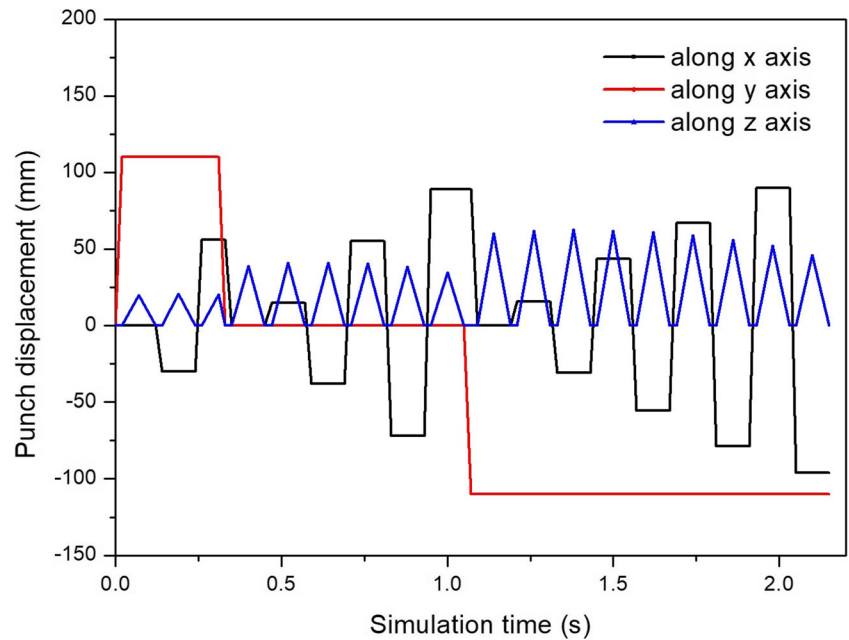
The experiment results in large single curvature metal plate bending are shown in Fig. 18. Figure 18 is the experimental bended metal plates at room temperature and 500 °C. The surface of the bended part appears smooth and there is no

visible dimples and wrinkles. Figure 18(b) shows the measured curve of the mid-line of the plates with a comparison of that of the designed curve. Figure 18(c) shows the error between the measured curves and designed curve. The maximum error is 5.8 mm and the average error is 2.4 mm at 500 °C. However, the maximum error is 15.3 mm and the average error is 11.2 mm at room temperature. It is noted that large errors occur near the quarter and middle part of the metal plates. This may be attributed to the fact that more plastic



Fig. 15 Experimental plates at various states. **a** Initial state. **b** First punching state. **c** Middle heating state. **d** Last state

Fig. 16 Loading trajectory of simulation in curved metal plate



deformation and displacement take place in the middle part of the metal plates for the large single curvature metal plate wherever the punching position is located in the incremental bending process, whereas this deformational behavior can be restrained by the heating method. In our previous study, the dimension of the deformed single curvature metal plates is

1000 mm × 800 mm, and the achieved radius curvature is only 2500 mm [9], while in this study, the achieved radius curvature for the single curvature metal plate is 180 mm, so the formability of the metal plates during the heat-assisted incremental bending process is greatly improved. The simulation results in large single curvature metal plate bending are shown

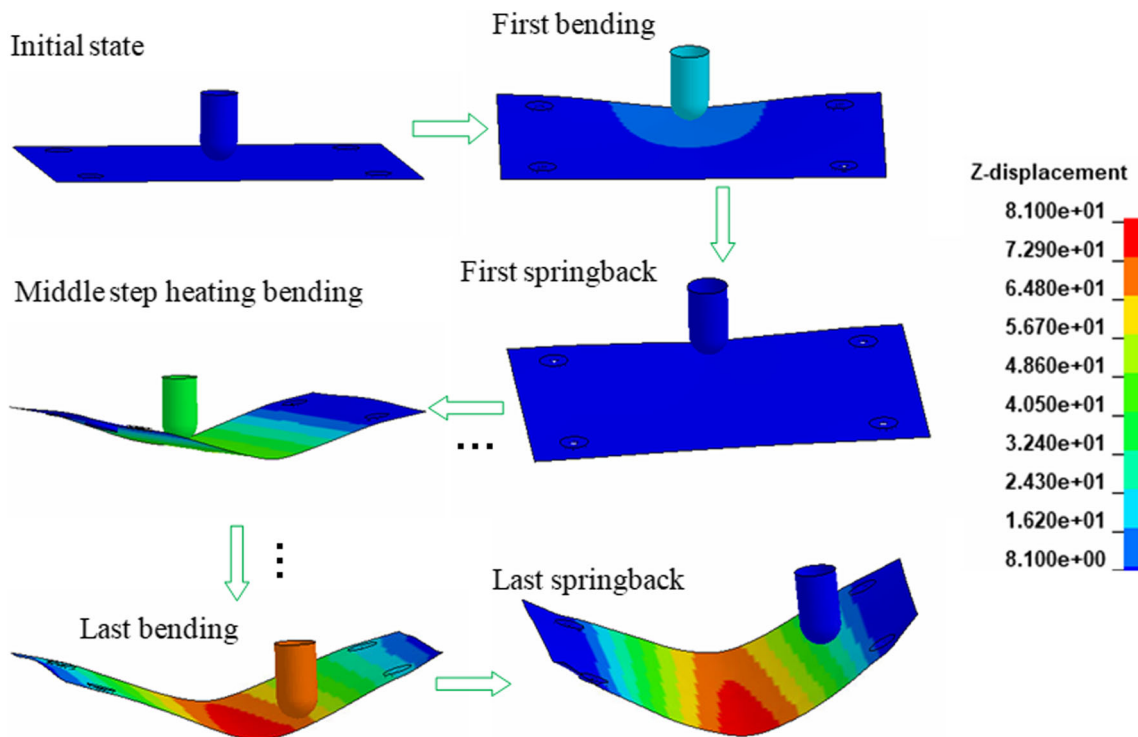


Fig. 17 Punching at various states during the whole heat-assisted incremental bending process

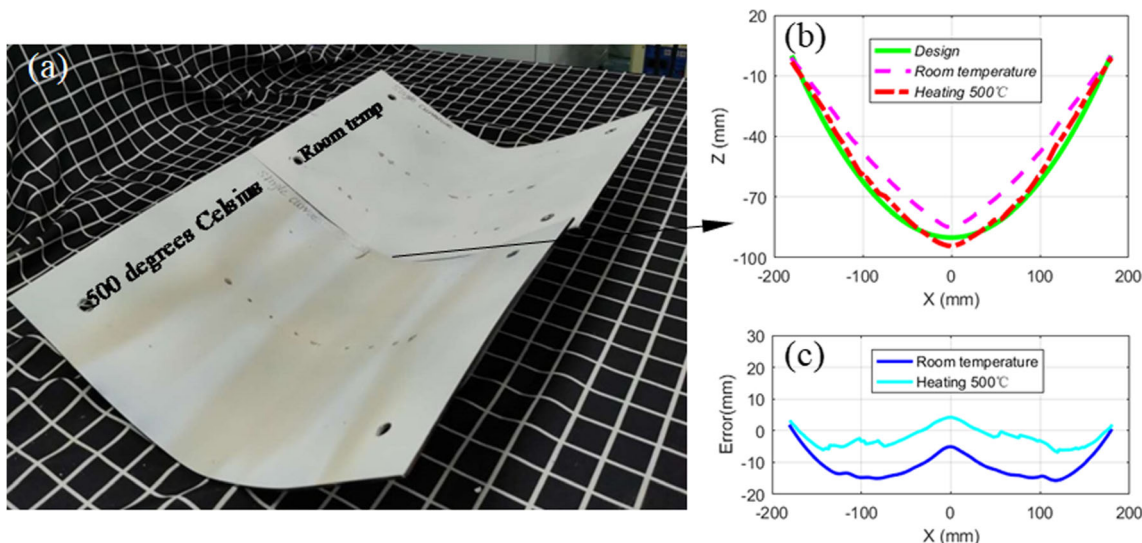


Fig. 18 Experimental results in large single curvature metal plate bending: (a) bending plates; (b) measured curves in the middle of the plate with a comparison the designed curve; (c) error between the designed curve and the measured curves

in Fig. 19. Figure 19(a) is the simulated results of the bended metal plates at room temperature and 500 °C. Figure 19(b) shows the simulation curve of the mid-line of the plates with a comparison of that of the designed curve. Figure 19(c) shows the error between the simulated curves and designed curve. Results show that there is a good consistency between the numerical simulation results and experimental results. The maximum relative error of numerical simulation is less than 10% for the case that are heated at 500 °C, so the numerical simulation results are validated. The slight difference between the experimental data and numerical ones may be caused by the simplification of support during the finite element numerical simulation. The error between the experiment, simulation curves, and designed curve reduce significantly when the metal plate was heated to 500 °C.

4.2 Analysis on the deformation behavior of metal plates with large variable curvature

The experiment results and the simulation results in large variable curvature metal plate bending are shown in Figs. 20 and 21. Figures 20b and 21b show the measured and simulated strip curves with a comparison to that of the designed strip curves. As we can see, the numerical simulation results also coincide well with the experimental data. Figures 20c and 21c show the errors. It can be found that the maximum error is 28.2 mm at room temperature. It is noted that large errors occur at the $Y = -110$ part of the metal plates. It is due to that there is a large effect of the neighboring strips for the large variable curvature metal plates at room temperature. As a comparison, the maximum error is 6.8 mm at 500 °C. It

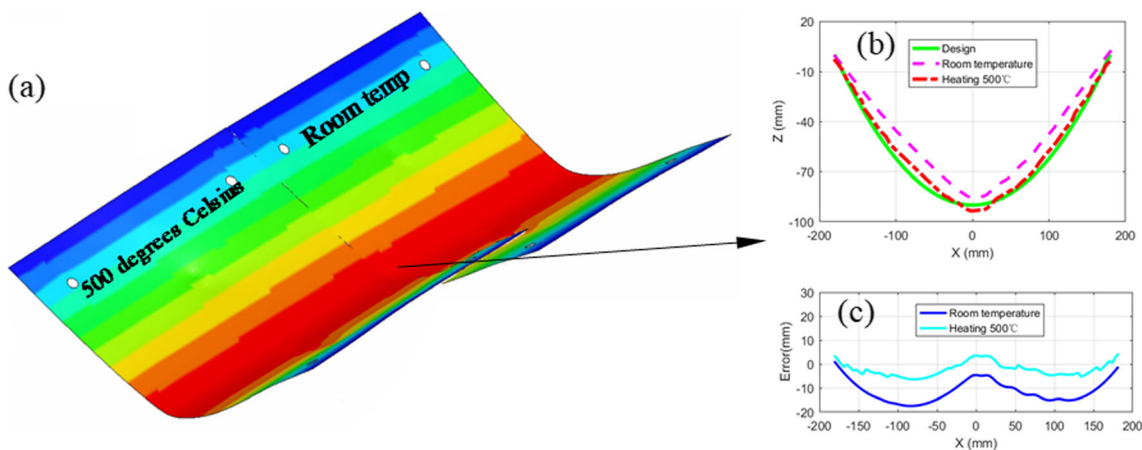


Fig. 19 The simulation results in large single curvature metal plate bending: (a) bending plates; (b) simulation curves in the middle of the plates with a comparison the designed curve; (c) error between the designed curve and the simulation curves

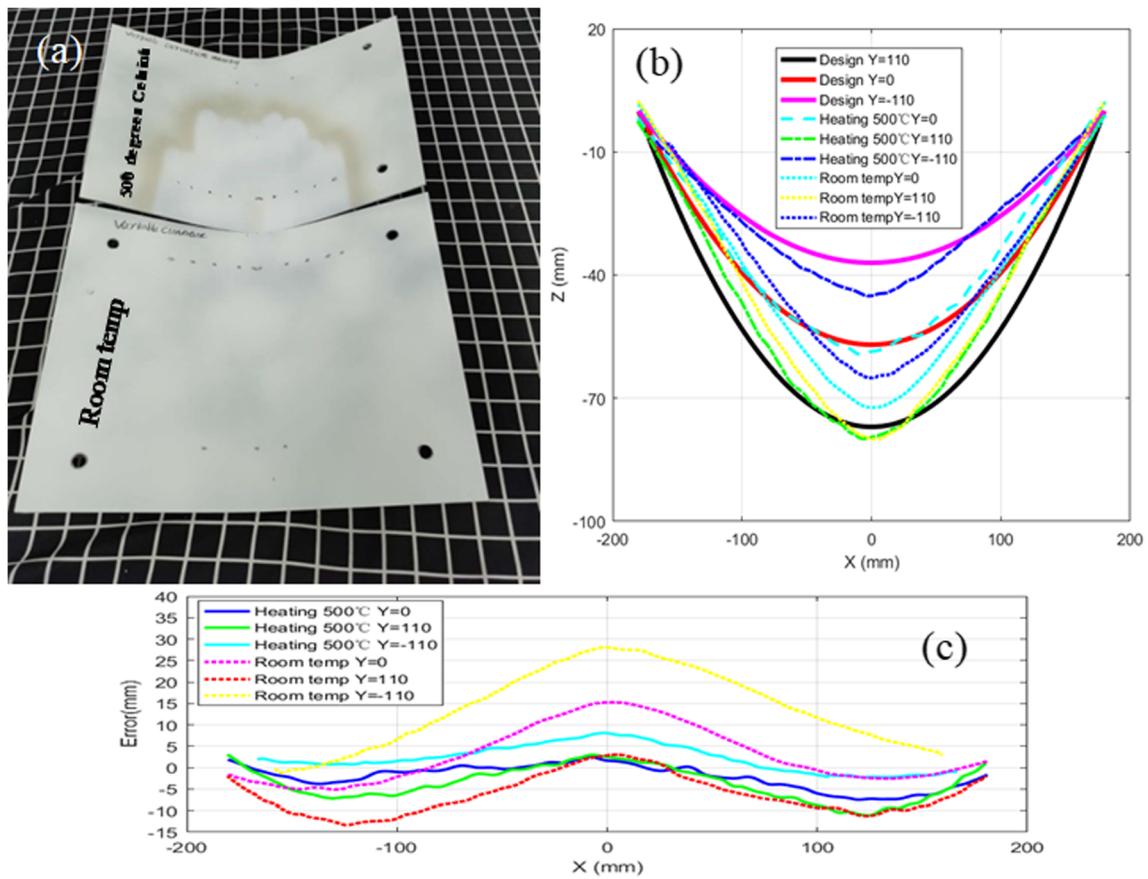


Fig. 20 Experimental results in large variable curvature metal plates bending: **a** bending plates; **b** measured curves of the three strips with a comparison to the designed curves; **c** error between the designed curve and the measured curves

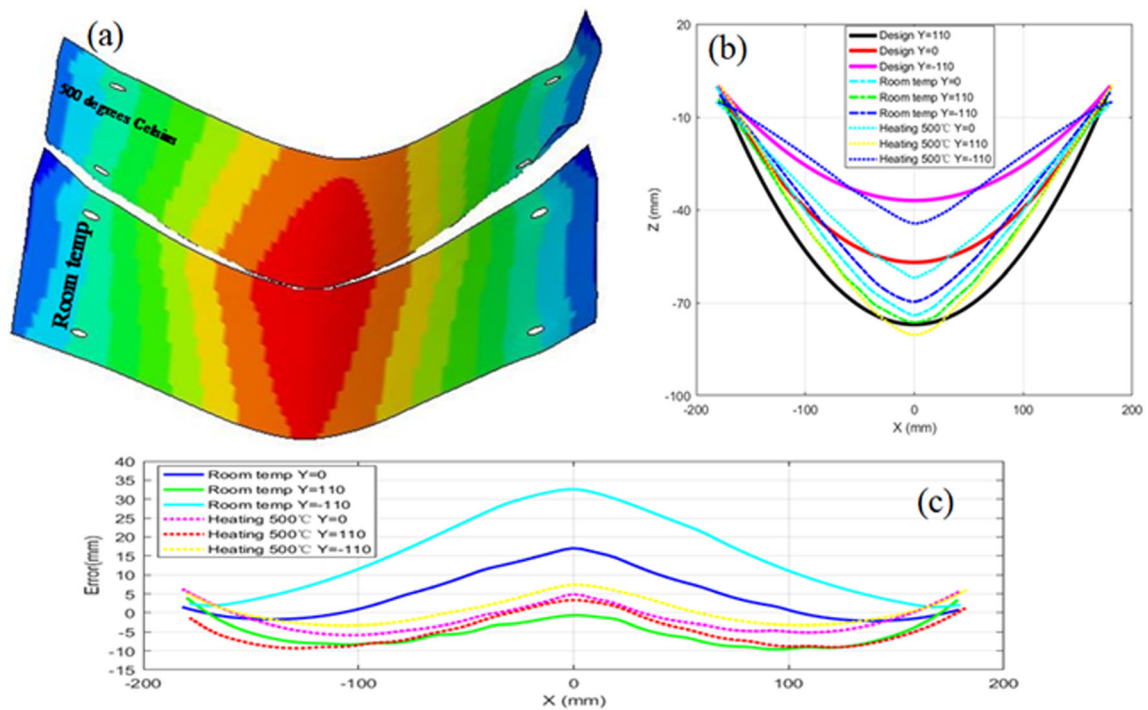


Fig. 21 Simulation result in large variable curvature metal plates bending: **a** bending plates; **b** simulated curves of the three strips with a comparison to the designed curves; **c** error between the designed curve and the simulated curves

demonstrates that the heating method is effective to reduce the effect of the neighboring strips. With a comparison of the previous experiment results [9], the radius curvature of the variable curved metal plate during the heat-assisted incremental bending process is decreased from 1785.7 to 202.5 mm.

5 Conclusions

In this paper, one novel heat-assisted incremental bending process was proposed to achieve metal plates with large curvature. In this method, the metal plate is supported by several supporting pillars and the punch moves according to the loading trajectory determined by the minimum energy method. In addition, the induction heating system is applied to heat the plates at the punching positions. The bending process continues step by step until the metal plate achieves the designed shape finally. The objective of this paper is to report the springback behavior and plastic deformation of the large curved metal plates during the heat-assisted incremental bending process and to provide a comprehensive explanation of the novel thermal-mechanical coupled sheet metal forming process based on theoretical analysis, numerical simulation, and experiments. The key conclusions are summarized as follows:

- 1) The heating temperature can greatly influence the punching force and springback behavior of the bending plates. The springback height of the Q235 steel plate is smaller than 2 mm when the temperature is 500 °C and punching depth is 60 mm.
- 2) The elastic-plastic-thermal coupled finite element model is validated by the corresponding heat-assisted incremental bending experiments. Thus, the finite element model can better guide the deformation process of the bending plate.
- 3) Comparison of the deformation results of the metal plates under different heating temperatures indicated that the heat-assisted incremental bending process can reduce the springback behavior and improve the deformation accuracy greatly.

In our future study, the new loading trajectory and heating method for the doubly curved metal plates that cannot be simply discretized into strips will be proposed.

Authors' contributions Bo Wei wrote the paper and carried out the experiments and numerical simulation; Yanan Wei helped with the experiments; Feifei Zhang helped with the framework of the paper and gave some data analysis and revision suggestions; Kai He provided the experimental condition; Xiaobing Dang provided the loading path determination method, Ruxu Du contributed to the main idea of combining heat and incremental bending.

Funding The research is supported by the SIAT-CUHK Joint Laboratory of Precision Engineering, SIAT Innovation Program for Excellent Young

Researchers (2019Y9G031), and Guangdong Basic and Applied Basic Research Foundation (2019A1515012035).

Data availability All data generated or analyzed during this study are included in this published article.

Compliance with ethical standards

Ethical approval and consent to participate No applicable

Consent to publish All authors have read and agreed to the published version of the paper.

Competing interests The authors declared that they have no competing interests.

References

1. Yu G, Anderson RJ, Maekawa T (2001) Efficient simulation of shell forming by line heating. *Int J Mech Sci* 43:2349–2370
2. Li MZ, Cai ZY, Sui Z, Yan QG (2002) Multi-point forming technology for sheet metal. *J Mater Process Technol* 129:333–338
3. Liu C, Li MZ, Fu W (2008) Principles and apparatus of multi-point forming for sheet metal. *Int J Adv Manuf Technol* 35:1227–1233
4. Peng H, Li MZ, Liu C, Cao J (2013) Study of multi-point forming for polycarbonate sheet. *Int J Adv Manuf Technol* 67:2811–2817
5. Su S, Hu Y, Wang C (2015) The key technology research about 3D CNC bending machine and experimental verification. *J Coast Res* 73:584–588
6. Luo YX, Yang WM, Liu ZF, Wang YQ, Du RX (2016) Numerical simulation and experimental study on cyclic multi-point incremental forming process. *Int J Adv Manuf Technol* 85:1249–1259
7. Luo YX, He K, Du RX (2010) A new sheet metal forming system based on the incremental punching, part 1: modeling and simulation. *Int J Adv Manuf Technol* 51:481–491
8. Luo YX, He K, Du RX (2010) A new sheet metal forming system based on incremental punching, part 2: machine building and experiment results. *Int J Adv Manuf Technol* 51:493–506
9. Dang XB, He K, Li W, Zuo QY, Du RX (2017) Incremental bending of three-dimensional free form metal plates using minimum energy principle and model-less control. *J Manuf Sci Eng* 139(7): 071009
10. Dang XB, He K, Zhang FF, Zuo QY, Du RX (2019) Multi-stage incremental bending to form doubly curved metal plates based on bending limit diagram. *Int J Mech Sci* 155:19–30
11. Wang C, Kinzel G, Altan T (1993) Mathematical modeling of plane-strain bending of sheet and plate. *J Mater Process Technol* 39:279–304
12. Yang X, Choi C, Sever NK, Altan T (2016) Prediction of springback in air-bending of Advanced High Strength steel (DP780) considering Young's modulus variation and with a piecewise hardening function. *Int J Mech Sci* 105:266–272
13. Khadra FA, El-Morsy AW (2016) Prediction of springback in the air bending process using a Kriging metamodel. *Eng Technol Appl Sci Res* 6(5):1200–1206
14. Dufloy JR, Callebaut B, Verbert J, De Baerdemaeker H (2007) Laser assisted incremental forming: formability and accuracy improvement. *CIRP Ann Manuf Technol* 56(1):273–276
15. Fan G, Gao L, Hussain G, Wu Z (2008) Electric hot incremental forming: a novel technique. *Int J Mach Tool Manu* 48:1688–1692

16. Ji YH, Park JJ (2008) Formability of magnesium AZ31 sheet in the incremental forming at warm temperature. *J Mater Process Technol* 201:354–358
17. Galdos L, Sáenz D, Argandoña E, Ulacia I, Arruebarrena G (2012) Warm incremental forming of magnesium alloys using hot fluid as heating media. *Key Eng Mater* 504-506:815–820
18. Gisario A, Barletta M, Venettacci S (2016) Improvements in springback control by external force laser-assisted sheet bending of titanium and aluminum alloys. *Opt Laser Technol* 86:46–53
19. Roohi AH, Gollo MH, Naeini HM (2012) External force-assisted laser forming process for gaining high bending angles. *J Manuf Process* 14:269–276
20. Hill R (1979) Theoretical plasticity of textured aggregates. *Math Proc Camb* 85:179–191
21. Safari M, Mostaan H (2016) Experimental and numerical investigation of laser forming of cylindrical surfaces with arbitrary radius of curvature. *Alex Eng J* 55:1941–1949

Publisher's note Springer Nature remains neutral with regard to jurisdictional claims in published maps and institutional affiliations.